Self-organized lane formation and optimized traffic flow in army ants

I. D. Couzin[1*] and N. R. Franks[2]

[1]*Department of Ecology and Evolutionary Biology, Princeton University, Princeton, NJ 08544, USA*
[2]*Centre for Behavioural Biology, School of Biological Sciences, University of Bristol, Bristol BS8 1UG, UK*

We show how the movement rules of individual ants on trails can lead to a collective choice of direction and the formation of distinct traffic lanes that minimize congestion. We develop and evaluate the results of a new model with a quantitative study of the behaviour of the army ant *Eciton burchelli*. Colonies of this species have up to 200 000 foragers and transport more than 3000 prey items per hour over raiding columns that exceed 100 m. It is an ideal species in which to test the predictions of our model because it forms pheromone trails that are densely populated with very swift ants. The model explores the influences of turning rates and local perception on traffic flow. The behaviour of real army ants is such that they occupy the specific region of parameter space in which lanes form and traffic flow is maximized.

Keywords: self-organization; mathematical model; computer simulation; social insects

1. INTRODUCTION

Networks that control the flow of resources and information are ubiquitous in nature. Moreover, the efficiency of such networks may determine the fundamental scaling properties of certain organisms (West *et al.* 1997; Banavar *et al.* 1999; Brown & West 2000). The foraging networks of terrestrial animal societies, and especially those of certain ant species, provide unrivalled opportunities to quantify both the behaviour of individual items of traffic and the larger-scale patterns of traffic flow. For these reasons, they are ideal subjects with which to test mathematical models that link the behaviour of small components (in this instance, individual ants) to the overall efficiency of the dynamic structures they generate.

Many ant species create chemical (pheromone) trail networks, not only to transport resources and/or information swiftly and efficiently during foraging, but also for exploration, emigration and coordinating colony defence (Hölldobler & Wilson 1990). Just as the functioning and success of modern cities are dependent on an efficient transportation system, the effective management of traffic is also essential to insect societies. The flow of traffic along trails is likely to be particularly important in the New World army ant *Eciton burchelli*. Colonies of this species may have half a million or more workers, and the ants are strict carnivores. They stage huge swarm raids, in pursuit of arthropod prey, with up to 200 000 virtually blind foragers forming trail systems that are up to 20 m wide and 100 m or more long (Schneirla 1971; Franks *et al.* 1991; Gotwald 1995; Solé *et al.* 2000). In a single such raid a colony may retrieve more than 30 000 prey items (Franks 1985). Moreover, these massive raids are severely time constrained. At most, they begin at dawn and end at dusk, when the colony emigrates, under the cover of darkness, to a new nest-site and foraging arena. For this reason, *E. burchelli* colonies need to operate at a very high tempo (see Franks *et al.* 1999; Boswell *et al.* 2001). These colonies form traffic lanes in their main foraging columns (Franks 1985). We investigate how and why these traffic lanes form. We first develop a generic model for trail following by ants, and compare the behaviour of the model with empirical data from individual ants following a trail of known concentration. We then parameterize this model with new data from an analysis of the movements of individual *E. burchelli* workers. We use this individual-based model to test theories concerning the organization of traffic on army ant trails, and demonstrate how individual behaviours lead to crucial properties including directionality, lane formation and the minimization of congestion.

2. THE MODEL

(a) *Overview*

We develop a general model of ant behaviour, using an individual-based simulation approach that takes into account the abilities of ants to detect and avoid colliding with one another and to respond to local pheromone concentration. N ants are simulated, with ant i having position vector $\mathbf{c}_i(t)$ and direction vector $\mathbf{v}_i(t)$. The head of ant i is at a point $\mathbf{c}_i(t) + 1/2\beta\mathbf{v}_i(t)$, where β is the ant body length. The left and right antennae each extend a distance ϕ from the head at an angle of 45° to the ant's body orientation. In the simulation, ants will turn away from others if they are approached too closely within either of two local areas. The first is a circle, radius r_d, extending from the ant's centre, $\mathbf{c}$, representing very close proximity to the body and legs of the ant. The second is an arc that extends ahead of the ant a distance r_p from $\mathbf{c}$ and has an internal angle α; this may represent a local visual field in some species, whereas in others (such as virtually blind army ants) it is the tactile range of the antennae or the close-range olfactory perception of other ants (figure 1*a*). Individuals tend to turn away from others within these zones with a turning rate θ_a (equation (2.1)), and also to slow down to avoid collisions with a constant acceleration, $-\mu$, unless they have already reached their minimum speed,

Proc. R. Soc. Lond. B (2003) **270**, 139–146
DOI 10.1098/rspb.2002.2210

139

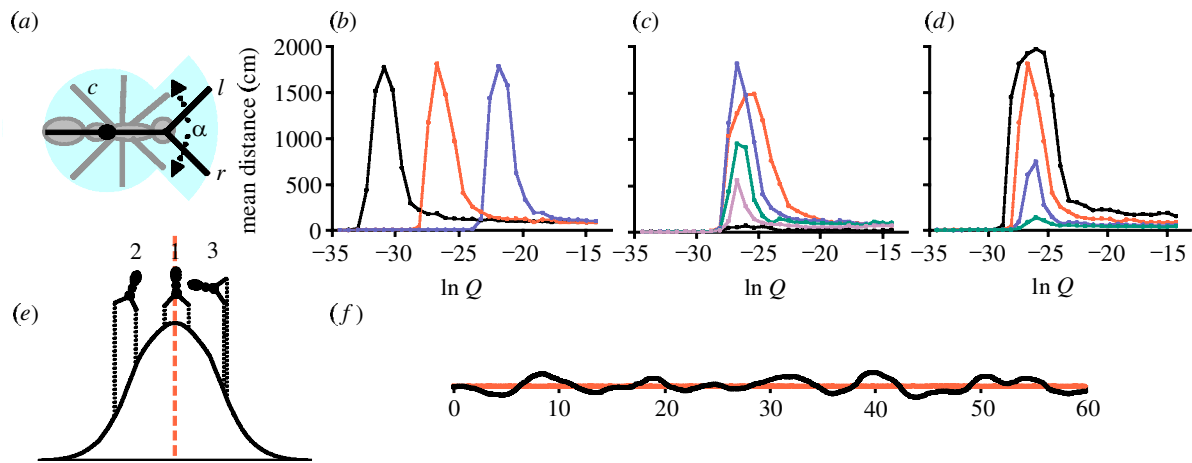*Author for correspondence (icouzin@princeton.edu).

Figure 1. (*a*) Geometry of simulated ants, showing the centre (*c*) the left and right antennae (*l* and *r*, respectively) and the behavioural zones, where α is the internal angle of the zone extending ahead of the ant. (*b*–*d*) The results of simulations showing the mean distance travelled as a function of the natural log of the amount of trail pheromone (ln *Q*). The results shown are the means of all runs for a given pheromone concentration, where ants approach the trail at angles of 5–90° (at 5° increments, 50 replicates per increment). Simulations were run for 15 000 time-steps per replicate (standard parameters: $\theta_p = 500°\,\text{s}^{-1}$, $\sigma = 0.5$, $C_{max} = 1.2 \times 10^{-10}\,\text{g cm}^{-3}$). (*b*) The saturation level of the antennae, C_{max}, changes the pheromone concentration at which the peak occurs because the response of the antennae is scaled according to this parameter. Values of C_{max} (in g cm^{-3}): black, 1.2×10^{-12}; red, 1.2×10^{-10}; blue, 1.2×10^{-8}. (*c*) Very low or high turning rates, θ_p, reduce the accuracy of trail following. If high, then ants can respond readily to pheromone gradients, but have a tendency to become perpendicular to the trail, which increases the probability of leaving (see *e*). If very low, ants respond slowly to gradients, which means they can only remain on a trail if they approach it from a shallow angle. However, once on a trail, error is less likely to result in them losing the trail since they turn slowly. At intermediate values trail-following ability is maximized. Values of θ_p (in degrees): black, 100; red, 300; blue, 500; green, 700; mauve, 900. (*d*) Increasing error reduces trail-following efficiency. Values of σ: black, 0.25; red, 0.5; blue, 0.75; green, 1.0. (*e*) The angle of an ant relative to the pheromone trail (here represented as the concentration profile) influences its ability to determine concentration gradients correctly. (*f*) Typical trajectories of simulated ants on a trail (units: cm) with no error (red) and with error in trail following (black).

u_{min}. When not avoiding collisions, ants respond to local concentrations of pheromone.

For mathematical tractability, we assume that ants follow a linear trail (equation (2.2)). *Q* is the amount of pheromone deposited, and simulated ants detect the concentration of pheromone at each of their antennal tips (figure 1*a*). In accordance with physiological studies on ants and other insects, the concentration at these points is converted into a 'stimulus intensity' (equation (2.3)). This stimulus increases rapidly as pheromone concentration increases, but the rate of increase decreases as the pheromone saturates the antennae (C_{max}). To simulate sensory error (e.g. sensory and/or environmental noise) the stimulus intensity is modified by adding a Gaussian-distributed random deviate centred on 0 with standard deviation σ. Ants turn towards the highest stimulus (perceived pheromone concentration) at turning rate θ_p. When ants are not avoiding collisions they accelerate with acceleration μ until they reach their desired speed u_{des}.

Time is partitioned into discrete steps, *t*, with spacing $\Delta t = 0.02$ s, chosen to match the temporal resolution of the experimental data. At each time-step, the direction vectors and then the position vectors of all ants are updated in parallel. The updating of the direction vectors is as follows (see § 2*b*–*d*).

(b) Interactions

If there are other ants, *j*, within the interaction zones of ant *i*, it avoids them by turning towards a desired vector

$$\mathbf{d}_i(t + \Delta t) = \sum_{j \neq i} \frac{\mathbf{c}_i(t) - \mathbf{c}_j(t)}{|(\mathbf{c}_i(t) - \mathbf{c}_j(t))|}. \tag{2.1}$$

The ant is able to turn through an angle of, at most, $\theta_a \Delta t$ degrees in time Δt; if the angle between $\mathbf{v}_i(t)$ and $\mathbf{d}_i(t + \Delta t)$ is less than $\theta_a \Delta t$, it achieves alignment with its desired vector, $\mathbf{v}_i(t + \Delta t) = \mathbf{d}_i(t + \Delta t)$, otherwise it turns $\theta_a \Delta t$ towards it.

(c) Pheromone

If there are no other ants within the interaction zones of ant *i*, it responds instead to pheromone concentration. This is a function of the radial distance, *r*, from the trail centre, which is symmetric with a maximum at $r = 0$. For an infinitely long line source and instantaneous emission, the concentration of pheromone *C* at diffusion time τ is

$$C(r,\tau) = \frac{Q}{2\pi D\tau}\exp\left(\frac{-r^2}{4D\tau}\right), \tag{2.2}$$

where *Q* is the amount of pheromone deposited (g cm^{-1}) and *D* is the diffusion coefficient ($D = 0.01$ cm^2 s^{-1}, approximating the typical diffusion constant of trail pheromone; Evershed *et al.* 1982; Calenbuhr & Deneubourg 1992; Calenbuhr *et al.* 1992). As we are interested here in the movement of ants along a pre-existing trail, we fix the concentration profile after set time τ, giving us the correct qualitative distribution of pheromone (Calenbuhr & Deneubourg 1992; Calenbuhr *et al.* 1992).

At a given point in time, the ant samples concentrations C_l and C_r at the ends of the left and right antennae, respectively. For each, this is converted into stimulus intensity

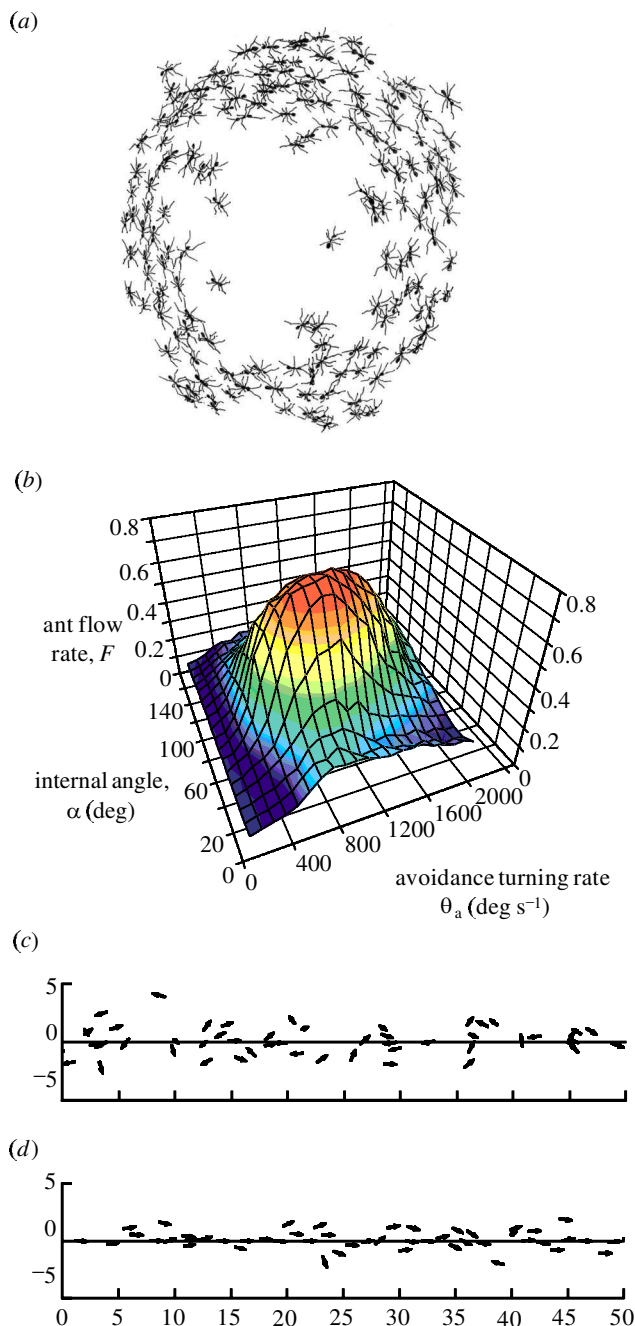$$S(C) = \frac{\tan^{-1}(k(C/C_{max}))}{\pi/2}, \tag{2.3}$$

and k is a constant that controls the rate at which the concentration approaches its maximal value ($k = 100$). S is limited to $0 \leqslant S \leqslant 1$. Ants turn in the direction of the highest perceived pheromone concentration by $\theta_p \Delta t$. If no concentration difference is detected, then $\theta_p = 0$. All turning is assumed to be subject to error. This is simulated by rotating $\mathbf{v}_i(t + \Delta t)$ by angle ε (a Gaussian-distributed random deviate centred on 0 with a standard deviation of 0.5 radians).

(d) Directional preference

In simulations where we investigate directional preference (see § 4(b)(ii)), we simulate it using a supplementary internal unit vector $\mathbf{g}_i(t + \Delta t)$ with weighting ω, and replacing $\mathbf{d}_i(t + \Delta t)$ by $\mathbf{d}_i'(t + \Delta t)$, where

$$\mathbf{d}_i'(t + \Delta t) = \frac{\mathbf{d}_i(t + \Delta t) + \omega\, \mathbf{g}_i(t + \Delta t)}{|\,\mathbf{d}_i(t + \Delta t) + \omega\, \mathbf{g}_i(t + \Delta t)\,|}. \tag{2.4}$$

This completes the description of the new direction vectors. The new position vector of ant i is then given by $\mathbf{c}_i(t + \Delta t) = \mathbf{c}_i(t) + \mathbf{v}_i(t + \Delta t)\Delta t\, u_i$, where u_i is the current speed of ant i.

We used our video analysis of the army ant *E. burchelli* (see § 3) to parameterize the model such that: $r_d = 0.4$ cm, $r_p = 1.2$ cm, $\beta = 0.8$ cm, $\phi = 0.4$ cm, $u_{des} = 13$ cm s^{-1}, $u_{min} = 2$ cm s^{-1} and $\mu = 50$ cm s^{-2}.

3. MATERIAL AND METHODS

Eciton burchelli raids were filmed in Panama (Soberania National Park). A section of the principal trail (11 cm long) was filmed from above using a digital video camcorder (Sony DVCAM). Owing to the high speed of these ants, we doubled the frame rate (from 25 to 50 Hz) by isolating both fields from each frame and interpolating the missing pixels from those above and below. This also sharpens the images, increasing spatial accuracy. The centre of each ant was then recorded, to allow reconstruction of trajectories. The acceleration and the minimum and maximum speeds of ants were calculated from the trajectories of 226 individuals. Owing to artefacts associated with analysis of trajectory data when using time to discretize trajectories (Tourtellot *et al.* 1991), the calculation of angular deviation as a result of interactions was standardized by recording the position of a focal ant in the first frame when it contacted another ant (usually antennal contact with the antennae, legs and/or body). Analysing the distance between ants during such initial contacts allowed us to estimate the interaction range, r_p. Using this as a reference point, a minimum distance interval (1.2 cm, approximately 1.5 body lengths) was specified. The position (centre) of the ant greater than, but closest to, this distance from the focal point before interaction was found. The line segment between these points (the point before interaction, the point where the focal ant interacts with another ant and the point after the interaction) gave the direction of the ant before interaction. The position of the ant after interaction was found using the same technique to determine the direction after interaction. The change in direction before and after interaction is the angular deviation. Similarly, this rule was used to calculate the angular deviation of simulated ants. For simplicity, we analysed only medium workers because these comprise 75% of all the ants in the raid (Franks 1985).

Figure 2. Circular milling. (*a*) Drawing of ants forming a circular mill in the laboratory (adapted from Schneirla 1971 by I.D.C.). (*b*) The flow of ants is dependent on their ability to detect others and the rate at which they turn during avoidance manoeuvres ($N = 50$, $\theta_p = 500°$ s^{-1}, $\sigma = 0.01$, $Q = 1.2 \times 10^{-6}$ g cm^{-3}, $C_{max} = 1.2 \times 10^{-6}$ g cm^{-3}, $\tau = 300$ s. F was calculated at $t = 5000$, and the results shown are the means of 100 runs per parameter combination). (*c*) Ants begin the simulation at random positions and with orientations along the trail. Snapshot near the start of a simulation ($t = 50$) with $\alpha = 90°$ and $\theta_a = 1000°$ s^{-1}. Ants are depicted as arrows representing their instantaneous velocity (units: cm). (*d*) Simulated ants have selected a direction collectively ($t = 3000$).

which is an increasing sigmoid function when C is on a log scale (Boeckh *et al.* 1984; Andryazak *et al.* 1990; Masson & Mustaparta 1990). C_{max} is the concentration at which the antennal receptors are completely saturated,

4. RESULTS

(a) *The behaviour of individual ants*

Initially, we investigated the behaviour of individual ants within the model in the absence of interactions with other ants. Before we can address how individual movements result in the coordination of a collective response, we must first consider how individuals interact with their local chemical environment. Laboratory studies have shown that the distance that an individual ant moves along a trail, before losing it, is a complex function of the pheromone concentration of that trail. Initially, as concentration increases, the length of trail that an ant can follow increases. However, as the concentration increases further, the trail-following ability begins to decrease, resulting in a distribution with a peak at intermediate pheromone concentration (Evershed *et al.* 1982; Pasteels *et al.* 1986; Calenbuhr *et al.* 1992). Furthermore, certain ant species exhibit a sinusoidal trajectory as the trail is followed (Hangartner 1967). The model replicates the peaked distribution of distance moved as a function of pheromone concentration, and shows how the parameters affect the shape of this distribution and the position of its peak (figure 1*b*–*d*). The saturation level, C_{max}, changes the position of the peak, with higher values of C_{max} moving the peak to the right (figure 1*b*). Turning rate, θ_p, also influences trail-following behaviour, with intermediate values maximizing the accuracy of trail following (figure 1*c*).

Error, σ, does not change the position of the peak, but increasing the error decreases the distance moved by ants before they lose a trail (figure 1*d*). Higher values of error increase fluctuations in the signal intensity detected by each antenna, resulting in a reduced effectiveness at differentiating the correct turning direction. Such noise has a greater influence on an ant's behaviour when there is only a slight difference in concentration between its antennae. This may occur when the ant is near the middle of the trail (figure 1*e*; ant 1), causing it to turn away from the centre. The concentration gradient increases as an ant leaves the centre (figure 1*e*; ant 2). Hence, the ant is able to move towards the centre again. The result is a sinusoidal trajectory (figure 1*f*). This is an inevitable consequence of individual error and need not be explicitly coded in the individual's behavioural response, as in a previous model (Calenbuhr & Deneubourg 1992; Calenbuhr *et al.* 1992). If pheromone concentration is very low and trails are very narrow, any error made by an ant is likely to cause it to lose a trail. As the concentration is increased, simulated ants become better able to follow the trail. However, if pheromone concentration is very high, there is sufficient space in the centre of the trail (where the pheromone gradient is shallowest) for errors to result in large changes in ant orientation relative to the trail direction. This can cause individuals to become perpendicular to the trail direction, reducing the difference in pheromone concentration detected by the antennae (figure 1*e*; ant 3). This increases the probability that an ant will leave the trail, an effect that is particularly strong if the centre of the trail is so concentrated that it saturates the antennae.

Certain army ants, unlike some other species (Hangartner 1967), show very little sinusoidal movement as they follow a trail, and this is likely to be because these ants exhibit very little error when detecting pheromone gradients. Low error is likely to be adaptive in this species, since the ants rely almost entirely on pheromone detection to remain within the swarm. In other, non-swarm-raiding, species, error may be adaptive in allowing ants to lose the trail system and, thereby, discover new food sources (Deneubourg *et al.* 1983).

(b) *The model applied to* Eciton burchelli

(i) *Collective selection of a direction*

We will now investigate the collective properties of the model during the generation of spatial pattern over a short but representative section of trail (equivalent to 50 cm). Army ants are not only good at following trails but also have a propensity to form circular mills when moderate numbers are separated from a colony and restricted to a confined area, either in the laboratory (figure 2*a*) or naturally in the field during exceptionally severe rainstorms (Schneirla 1971; Franks *et al.* 1991; Gotwald 1995). After a period of disorder, the ants all begin moving in the same direction. This behaviour is likely to reflect the ability of army ant colonies collectively to select a raid direction. We use periodic boundary conditions, which make the simulation very similar to the circular mill, and investigate how the model parameters influence the collective behaviour of ants on the trail section.

The flow of simulated ants, F, (measured as the normalized magnitude of the sum of the velocities of all individuals; values close to 0 represent little flow in a given direction, and those close to 1 represent high flow in one direction) is influenced strongly by the avoidance turning rate, θ_a, and the internal angle of the perception zone ahead of an ant, α (figure 2*b*). High flow rates occur when the ants select a direction collectively (figure 2*c,d*). When θ_a is low, ants require repeated collisions with others before their trajectory is influenced strongly enough for them to turn around. This causes congestion because ants turn slowly when they detect others, and, consequently, must slow down to avoid collisions. Conversely, when θ_a is very high, ants change direction very quickly when others are detected, and their orientations do not become correlated. Similarly, when α is low, ants cannot detect others ahead of them adequately, and are thus relatively insensitive to the positions of others. If α is high, however, they spend much of their time avoiding individuals that they would be unlikely to collide with. At intermediate values of these parameters ants are sufficiently sensitive, yet not overly sensitive, to the positions of others and, consequently, can select a direction collectively (hereafter $\alpha = 90°$). In this region of parameter space stochastic fluctuations in the number of ants travelling in each direction leads to one direction being more common than the other. This change causes an autocatalytic behavioural response as ants opposing the main flow are forced to turn around through repeated head-on interactions. As more ants move in one direction, it becomes increasingly hard for individuals to move the opposite way, and this causes the ants collectively to select a (randomly determined) direction.

(ii) *Bi-directional traffic and lane formation*

The results of the model suggest that army ants have evolved a behavioural response that results in a general

tendency for them to all move in the same direction along a trail. Under natural conditions, certain army ants exhibit a predominantly unidirectional flow of workers away from the nest in the first stage of a raid, but, as an increasing number of ants return to the nest carrying prey, the flow of ants in the raiding columns becomes bi-directional (Schneirla 1971; Gotwald 1995). Yet, such stable bi-directionality has not been observed in circular mills (Schneirla 1971; Franks *et al.* 1991; Gotwald 1995). When returning or outbound army ants are made to perform a U-turn on a natural raid trail, they quickly revert to their former orientation independently of tactile interactions with other ants (Gotwald 1995; I. D. Couzin, unpublished data). These observations and the model suggest that individual army ants, in a real raid, have a sense of direction.

In the sections of principal trails of the army ant *E. burchelli* that we filmed, the ants exhibited a distinct spatial structuring, with ants leaving the nest predominantly using both margins of the trail and ants returning to the nest using the centre (figure 3*a*). A similar three-lane system has also been described in termites (Jander & Daumer 1974). To understand how and why this pattern exists, we recorded the trajectories of 113 outbound and 113 inbound ants before, during and after they had interacted with one another (constituting 113 separate collision events). Figure 3*b* shows the trajectory of a single returning ant (grey) interacting with outbound ants (black). This demonstrates a qualitative difference in behaviour between the two types of ants, with those leaving the nest appearing to exhibit a higher rate of turning during avoidance manoeuvres than do returning ants. The change in direction of ants is very rapid (successive points are 0.02 s apart). To quantify this difference, we recorded the changes in angle of ant trajectories as a result of avoidance manoeuvres, and again found a difference between outbound ants and those returning to the nest, with returning ants exhibiting a lower turning rate (figure 3*c*).

How do *E. burchelli* army ants form traffic lanes? Can this difference in turning rate account for the pattern seen? We assume that the ants have a sense of direction (Gotwald 1995). Hence, each simulated ant is now supplied with a supplementary internal directional vector (equation (2.4)) that is parallel to the trail, pointing either to the left (returning towards a 'nest') or to the right (outbound towards a 'foraging area'). $N/2$ ants have a preference to move in each direction, weighted by a factor ω. Hence, the future direction chosen by an ant is a combination of the result of the social forces described previously and the propensity to move towards or away from the nest. If $\omega = 0$, ants have no directional preference; whereas, if $\omega = 1$, they balance directional preference and local (pheromone or tactile) conditions equally. As ω is increased above 1 the directional preference outweighs the local conditions. We also assume that outbound ants have a higher avoidance turning rate than those returning; the difference being $\Delta\theta_a$.

To quantify the flow of ants on bi-directional trails, the flow parameter, F, was calculated independently for ants returning to and leaving the nest. We found that the rate of flow of each group in their desired direction is strongly correlated, so here F is the numerical average of that calculated for each group. F is dependent on the strength of directional preference, ω, and the magnitude of the asymmetry of avoidance turning rate, $\Delta\theta_a$, between outbound and returning ants (figure 4*a*). Regardless of $\Delta\theta_a$, F is maximized when $\omega = 1$ (i.e. ants equally balance local conditions with their directional preference). When ω approaches 0, ants have only a small tendency to move in a given direction, and F is consequently low; whereas, when ω is high, ants rarely engage in avoidance manoeuvres, resulting in congestion as ants are forced to slow down through long-lasting collisions. At intermediate values, increasing $\Delta\theta_a$ causes an asymptotic increase in F. This increase corresponds to the emergence of a distinct spatial structuring of ants on the trail, with returning ants occupying the centre of the trail and outbound ants occupying the periphery (figure 4*a*, inset). To compare the model with the experimental data, we recorded the distribution of simulated ants relative to the trail centre (figure 4*b*–*d*) and also their angular deviation after interaction (figure 4*e*–*g*) using the same criteria as for real ants. In the area of parameter space in which flow is maximized, the results of the model are very similar to those obtained experimentally (cf. simulated figure 4*b*,*e* with experimental figure 3*a*,*c*).

5. DISCUSSION

Trail laying allows social insects to coordinate group responses over large temporal and spatial scales. The macroscopic properties of trail structures, such as their shape or the rate of recruitment to food sources, have been studied both empirically (Deneubourg *et al.* 1986, 1990; Pasteels *et al.* 1987; Deneubourg & Goss 1989; Goss *et al.* 1989; Beckers *et al.* 1990; Franks *et al.* 1991; Beekman *et al.* 2001) and through the use of mathematical models and simulations (Goss & Deneubourg 1989; Deneubourg *et al.* 1989; Stickland *et al.* 1993, 1995; Britton *et al.* 1998; Nicolis & Deneubourg 1999; Beekman *et al.* 2001). However, little is known about the microdynamics of these structures (the movement of individual ants), and the majority of previous approaches neglect the influence of direct interactions between individuals. Using a combination of detailed analyses of individual motion and the development of individual-based computer models, we have shown that local interactions and individual movement rules can strongly influence the organization of traffic over a large spatial scale.

Our model reveals how individual ants follow chemical trails and that simple and local rules can account for the ability of army ants collectively to select a direction on a given section of trail. Furthermore, we show how an asymmetry in turning rate (during interactions with others) between outbound and returning army ants can generate a three-lane structure, in which returning ants occupy the central lane on bi-directional trails. This acts to reduce the number of high-speed collisions between ants moving in different directions, and, consequently, increases the flow of ants to and from the nest.

Lane formation is also known to emerge spontaneously in human crowds under certain conditions. Where there is bi-directional traffic (such as on a walkway or crosswalk) 'bands' of pedestrians can form, each band composed of pedestrians with a common directional preference (Milgram & Toch 1969). These large-scale patterns are
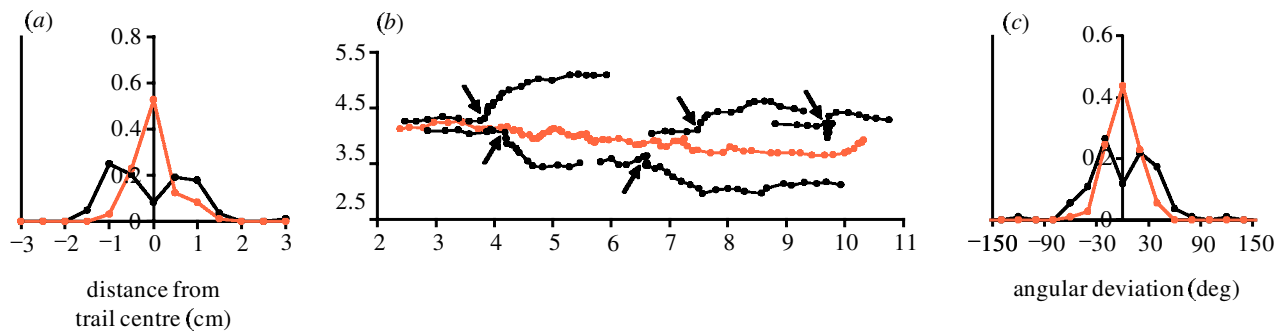
Figure 3. Experimental study of *E. burchelli* traffic organization. Returning ants in red, and outbound ants in black. (*a*) The proportion of ants as a function of distance from the trail centre (returning $N = 97$, outbound $N = 84$). (*b*) Trajectories of workers, showing a returning ant (moving to the left) interacting with five outbound ants (moving to the right). The arrows indicate where interactions occurred (units: cm). (*c*) The proportion of angular deviations exhibited by ants as a result of avoidance manoeuvres ($N = 113$ interactions, 226 ants).
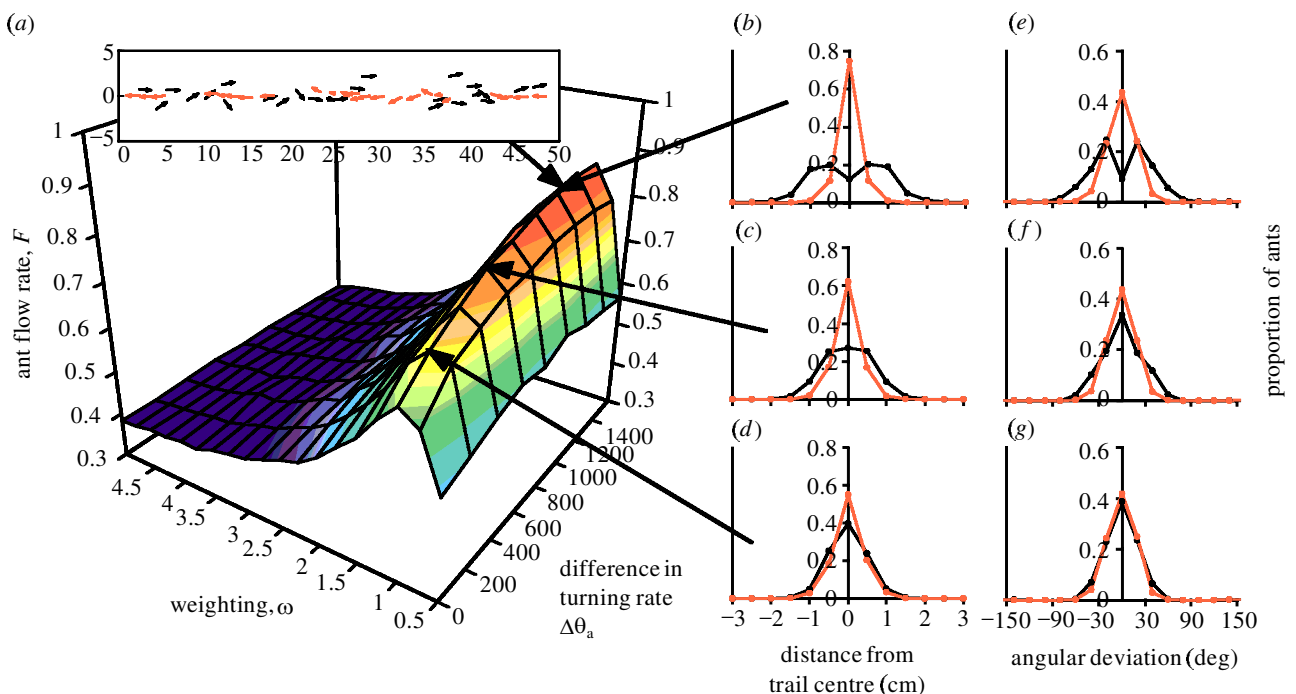

Figure 4. Simulation of ants on bi-directional trails. (*a*) The rate of movement of ants along a trail, *F*, as a function of the directional preference, ω, and asymmetry of the avoidance turning rate, θ_a (parameters as for figure 2). Inset, snapshot of the simulation in the area of parameter space where *F* is maximized, showing returning ants (red) tending to occupy the centre of the trail and outbound ants (black) tending to occupy the periphery (units: cm). (*b*–*d*) Distribution of ants from the trail centre at $\Delta\theta_a = 1400°\,\mathrm{s}^{-1}$, $600°\,\mathrm{s}^{-1}$ and $200°\,\mathrm{s}^{-1}$, respectively. Results calculated at $t = 5000$, and the means of 100 replicates shown. (*e*–*g*) Angular deviations of ants after avoidance manoeuvres at $\Delta\theta_a = 1400°\,\mathrm{s}^{-1}$, $600°\,\mathrm{s}^{-1}$ and $200°\,\mathrm{s}^{-1}$, respectively. Results shown are from the first 5000 interactions when $t > 5000$.

seldom evident to an individual pedestrian because they often have a limited perceptive radius in which information to determine future movement must be gathered. Like army ants, pedestrians in crowds balance goal-oriented behaviour (desire to reach a destination) with local conditions created by the motion and positions of nearby pedestrians (avoidance of collisions). It is the balance of these 'social forces' that results in lane formation. Individuals meeting others head-on will have 'strong' interactions in which they are likely to slow down and turn away to avoid collisions. Individuals that find themselves behind others moving in the same direction as themselves are less likely to perform such extreme avoidance manoeuvres, and, in turn, they 'protect' others behind

them from head-on avoidance moves, increasing the flow rate. Thus, given a sufficient density of pedestrians, they will spontaneously form lanes (Helbing & Molnár 1995).

The number of lanes that form in human crowds scales linearly with the width of the walkway (Helbing & Molnár 1995). Thus, there is a characteristic length-scale to this pattern-forming process: that is, from any point in the system statistically similar motions occur one wavelength (lane width) away (in the direction perpendicular to the desired motion). This is in contrast to the fixed three-lane system of army ants, which results from the asymmetry in interactions (absent in human crowds) combined with a tendency for all ants to move towards the highest concentration of pheromone. A further difference between ants

and humans is that pedestrians can typically be expected to behave selfishly. That is, they will tend to minimize their own travel time, but this may be at the cost of others. An army ant colony, however, is composed of cooperative individuals. Thus, natural selection can build an adaptive pattern at the global level by selecting and modifying individual rules that encode collective patterns. The asymmetry in interactions we have revealed is therefore likely to have been selected for. However, there is another potential explanation that is not mutually exclusive: many ants returning to the nest are burdened with prey, and this may make them less manoeuvrable than unladen ants leaving the nest.

Why do army ants have a three-lane structure as opposed to one with just two lanes? The latter organization may further increase traffic flow by reducing the interface between ants moving in different directions along a trail and, hence, minimizing time-consuming head-on interactions. Such two-lane traffic flow can be simulated by incorporating a bias in turning direction during interactions, such that all ants predominantly turn either clockwise or anticlockwise. However, a two-lane structure introduces an asymmetry into the trail system, and this 'handedness' in the extended phenotype (swarm) is likely to limit its overall efficiency (for example by biasing the ability of ants to raid to one side or another from a central trail). Another probable reason why two lanes would not be advantageous is that returning ants are thought to deposit more pheromone than outbound ants (Deneubourg *et al.* 1989). Thus, given that all ants exhibit a tendency to move towards the highest pheromone concentration, a two-lane system would not be spatially stable: outbound ants would have a tendency to drift to the side where ants return, forcing these ants further to that side, and so on.

Although lane formation has been observed in some termite species (Jander & Daumer 1974; Miura & Matsumoto 1998), the Neotropical army ants *Eciton hamatum* (Schneirla 1971) and *E. burchelli*, and African driver ants of the genus *Dorylus*, other ant species with dense traffic, such as the leafcutter ant *Atta cephalotes*, that may be expected to benefit from lanes do not exhibit this collective behaviour (Burd *et al.* 2002). It is possible that this is because leafcutter ants are less time constrained during foraging than army ants, and they do exhibit a much slower tempo. Nevertheless, one would expect that reducing travel time should benefit any central-place forager. Burd *et al.* (2002), for example, showed that the mingling of outbound and returning traffic on *Atta* trails reduced the speed of ants by an average of 16% relative to speeds on collision-free sections of trail. They suggested that these ants may benefit from information transfer during collisions. The most plausible explanation, which was also suggested by Burd *et al.* (2002), is that in *Atta* there is likely to be a greater difference in the returning speeds of different individuals than in *E. burchelli*, which is known to exhibit a highly consistent retrieval speed, facilitating the smooth flow of returning traffic (Franks 1985). In *Atta* constraints may be imposed by the size and shape of their loads (vegetation, typically leaf fragments). Laden leafcutter ants appear much less manoeuvrable than army ants, which can sling their relatively high mass-to-surface-area loads (arthropod prey) under their bodies. The bene-

fit of having lanes, which would seem to be hypothetically possible for *Atta* if individuals cut leaves to smaller sizes, presumably does not exceed the cost incurred by reducing the load per returning ant. This possible constraint to manoeuvrability in *Atta* may mean that, if they did form lanes, the slowest individuals would limit the speed of returning ants within their lane. The testing of such theories would benefit from a combination of experimental and modelling approaches, such as that we adopt here.

In summary, the combination of our new model and observations of ant behaviour demonstrates how individuals follow trails, and how direct small-scale interactions between individuals can lead to sophisticated self-organized structures, such as collectively selected unidirectional flow and multiple, minimally congested, traffic lanes.

REFERENCES

Andryzak, N. A., Payne, T. L., Dickens, J. C., Moser, J. C. & Fisher, R. W. 1990 Antennal olfactory responsiveness of the Texas leaf cutting ant (Hymenoptera: Formicidae) to trail pheromone and its two alarm substances. *J. Entomol. Sci.* **25**, 593–600.

Banavar, J. R., Maritan, A. & Rinaldo, A. 1999 Size and form in efficient transportation networks. *Nature* **399**, 130–132.

Beckers, R., Deneubourg, J. L., Goss, S. & Pasteels, J. M. 1990 Collective decision making through food recruitment. *Insect. Soc.* **37**, 258–267.

Beekman, M., Sumpter, D. J. T. & Ratnieks, F. L. W. 2001 A phase transition between disordered and ordered foraging in Pharoah's ants. *Proc. Natl Acad. Sci. USA* **98**, 9703–9706.

Boeckh, J., Distler, P., Ernst, K. D., Hösl, E. M. & Malun, D. 1984 Olfactory bulb and antennal lobe. In *Chemosensory information processing* (ed. D. Schild), pp. 201–228. Heidelberg: Springer.

Boswell, G. P., Franks, N. R. & Britton, N. F. 2001 Arms races and the evolution of big fierce societies. *Proc. R. Soc. Lond.* B **268**, 1723–1730. (DOI 10.1098/rspb.2001.1671.)

Britton, N. F., Stickland, T. R. & Franks, N. R. 1998 Analysis of ant foraging algorithms. *J. Biol. Syst.* **6**, 315–336.

Brown, J. H. & West, G. B. 2000 *Scaling in biology*. Oxford University Press.

Burd, M., Archer, D., Aranwela, N. & Stradling, D. J. 2002 Traffic dynamics of the leaf-cutting ant, *Atta cephalotes*. *Am. Nat.* **159**, 283–293.

Calenbuhr, V. & Deneubourg, J.-L. 1992 A model for osmotropotactic orientation. I. *J. Theor. Biol.* **158**, 359–393.

Calenbuhr, V., Chrétien, L., Deneubourg, J.-L. & Detrain, C. 1992 A model for osmotropotactic orientation. II. *J. Theor. Biol.* **158**, 395–407.

Deneubourg, J. L. & Goss, S. 1989 Collective patterns and decision-making. *Ethol. Ecol. Evol.* **1**, 295–311.

Deneubourg, J. L., Pasteels, J. M. & Verhaeghe, J. C. 1983 Probabilistic behaviour in ants: a strategy of errors? *J. Theor. Biol.* **105**, 259–271.

Deneubourg, J. L., Aron, S., Goss, S., Pasteels, J. M. & Duerink, G. 1986 Random behaviour, amplification processes and number of participants: how they contribute to the foraging properties of ants. *Physica* D **22**, 176–186.

Deneubourg, J. L., Goss, S., Franks, N. R. & Pasteels, J. M. 1989 The blind leading the blind: modelling chemically mediated army ant raid patterns. *J. Insect Behav.* **2**, 719–725.

Deneubourg, J. L., Aron, S., Goss, S. & Pasteels, J. M. 1990 The self-organising exploratory pattern of the Argentine ant. *J. Insect Behav.* **3**, 159–168.

Evershed, R. P., Morgan, E. D. & Cammaerts, M. C. 1982 3-ethyl-2,5-dimethyl-pyrazine, the trail pheromone from the venom gland of eight species of *Myrmica*. *Insect Biochem.* **12**, 383–395.

Franks, N. R. 1985 Reproduction, foraging efficiency and worker polymorphism in army ants. In *Experimental behavioural ecology* (ed. B. Hölldobler & M. Lindauer), pp. 91–107. Stuttgart: G. Fisher.

Franks, N. R., Gomez, N., Goss, S. & Deneubourg, J.-L. 1991 The blind leading the blind in army ant raid patterns: testing a model of self-organisation (Hymenoptera: Formicidae). *J. Insect Behav.* **4**, 583–607.

Franks, N. R., Sendova-Franks, A. B., Simmons, J. & Mogie, M. 1999 Convergent evolution, superefficient teams and tempo in Old and New World army ants. *Proc. R. Soc. Lond.* B **266**, 1697–1701. (DOI 10.1098/rspb.1999.0834.)

Goss, S. & Deneubourg, J. L. 1989 The self-organising clock pattern of *Messor pergandei*. *Insect. Soc.* **36**, 339–376.

Goss, S., Aron, S., Deneubourg, J. L. & Pasteels, J. M. 1989 Self-organised shortcuts in the argentine ant. *Naturwissenschaften* **76**, 579–581.

Gotwald, W. H. 1995 *Army ants: the biology of social predation*. Ithaca, NY: Cornell University Press.

Hangartner, W. 1967 Spezifität und inaktivierung des spurpheromons von *Lasius fuliginosus* (Latr.) und orientierung der arbeiterinnen im duftfeld. *Z. vergl. Physiol.* **57**, 103–136.

Helbing, D. & Molnár, P. 1995 Social force model for pedestrian dynamics. *Phys. Rev.* E **51**, 4282–4286.

Hölldobler, B. & Wilson, E. O. 1990 *The ants*. Berlin: Springer.

Jander, R. & Daumer, K. 1974 Guide-line and gravity orientation of blind termites foraging in the open (Termitidae: Macrotermes, Hospitalitermes). *Insect. Soc.* **21**, 45–69.

Masson, C. & Mustaparta, H. 1990 Chemical information processing in the olfactory system of insects. *Physiol. Rev.* **70**, 199–245.

Milgram, S. & Toch, H. 1969 Collective behaviour: crowds and social movements. In *The handbook of social psychology* (ed. G. Lindzey & E. Aronson), pp. 507–610. Reading, MA: Addison-Wesley.

Miura, T. & Matsumoto, T. 1998 Open-air litter foraging in the nasute termite *Longipeditermes longipes* (Isoptera: Termitidae). *J. Insect Behav.* **11**, 179–189.

Nicolis, S. C. & Deneubourg, J. L. 1999 Emerging patterns and food recruitment in ants: an analytical study. *J. Theor. Biol.* **198**, 575–592.

Pasteels, J. M., Deneubourg, J.-L., Verhaeghe, J.-C., Boevé, J.-L. & Quinet, Y. 1986 Orientation along terrestrial trails by ants. In *Mechanisms in insect olfaction* (ed. J. M. Pasteels & J. L. Deneubourg), pp. 155–175. Oxford: Clarendon Press.

Pasteels, J. M., Deneubourg, J. L. & Goss, S. 1987 Self-organisation mechanisms in ant societies. I. Trail recruitment to newly discovered food sources. In *From individual to collective behaviour in the social insects* (ed. J. M. Pasteels & J. L. Deneubourg), pp. 155–174. Basel: Birkhauser.

Schneirla, T. C. 1971 *Army ants: a study in social organisation*. San Francisco, CA: Freeman.

Solé, R. V., Bonabeau, E., Delgado, J., Fernandez, P. & Martin, J. 2000 Pattern formation and optimisation in army ant raids. *Artificial Life* **6**, 219–227.

Stickland, T. R., Tofts, C. & Franks, N. R. 1993 Algorithms for ant foraging. *Naturwissenschaften* **80**, 427–430.

Stickland, T. R., Britton, N. F. & Franks, N. R. 1995 Complex trails and simple algorithms in ant foraging. *Proc. R. Soc. Lond.* B **260**, 53–58.

Tourtellot, M. K., Collins, R. D. & Bell, W. J. 1991 The problem of movelength and turn definition in analysis of orientation data. *J. Theor. Biol.* **150**, 287–297.

West, G. B., Brown, J. H. & Enquist, B. J. 1997 A general model for the origin of allometric scaling laws in biology. *Science* **276**, 122–126.